Accurate Measurement of the Exciton Diffusion Length in a Conjugated Polymer Using a Heterostructure with a Side-Chain Cross-Linked Fullerene Layer

Denis E. Markov,*,† Emiel Amsterdam,† Paul W. M. Blom,† Alexander B. Sieval,‡ and Jan C. Hummelen†

Molecular Electronics, Materials Science Centre^{Plus}, University of Groningen, Nijenborgh 4, 9747 AG Groningen, The Netherlands, and Biomade Technology Foundation, Nijenborgh 4, 9747 AG Groningen, The Netherlands

Received: February 24, 2005; In Final Form: April 22, 2005

Exciton diffusion and photoluminescence quenching in conjugated polymer/fullerene heterostructures are studied by time-resolved photoluminescence. It is observed that heterostructures consisting of a spin-coated poly(*p*-phenylene vinylene) (PPV)-based derivative and evaporated C_{60} are ill-defined because of diffusion of C_{60} into the polymer, leading to an overestimation of the exciton diffusion length. This artifact is resolved by the use of a novel, thermally side-chain polymerizing and cross-linking fullerene derivative (F2D) containing two diacetylene moieties, forming a completely immobilized electron acceptor layer. With this heterostructure test system, an exciton diffusion length of 5 ± 1 nm is derived for this PPV derivative from time-integrated luminescence quenching data.

1. Introduction

Photovoltaic devices based on conjugated polymers and fullerenes[1,2] are attractive because of their mechanical flexibility and simple and potentially low-cost fabrication.[3] The most efficient solar cells, based on bulk heterojunctions of poly(*p*-phenylene vinylene)s (PPVs) and fullerene derivatives, have a characteristic power-conversion efficiency of 2.5[4]−3%[5] and incident-photon-to-collected-electron efficiency of around 50%.[6] The photoactive layer of these solar cells consists of an interpenetrating network of conjugated polymer and fullerene, with a polymer fraction of no more than 25 wt %.[7] This relatively small fraction is responsible for a main portion of the light absorption, since the most widely used [60]fullerene derivatives, like [6,6]-phenyl C_{61} butyric acid methyl ester (PCBM), have a low absorption coefficient in the visible range of the spectrum. After photoexcitation of the polymer phase, the photoexcitations migrate toward the polymer/fullerene interface where electron transfer from the polymer (donor) to the fullerene (acceptor) takes place. In poly[2-methoxy-5-(3′,7′-dimethyloctyloxy)-*p*-phenylene vinylene] (MDMO−PPV): PCBM blends, this electron transfer occurs within tens of femtoseconds, whereas the back transfer is in the millisecond range.[8] Consequently, the diffusion of excitons toward the polymer/fullerene heterojunction is an important process with regard to the efficiency of the device. The exciton diffusion length determines the size of the polymer phase that is effective in the charge carrier generation process. Enhanced exciton diffusion allows for larger polymer domains, hence for an increase of the fraction of polymer in the blend, which in turn gives rise to an increased absorption (in the case of a weakly absorbing acceptor).

The exciton diffusion lengths in various conjugated polymers reported in the literature show a large variation, ranging from 5 to 14 nm.[9−12] Most of these studies make use of a bilayer model system, comprising an evaporated C_{60} layer in combination with a conjugated polymer, spin-coated from solution. Comparatively, from photocurrent measurements on precursor PPV/C_{60} photovoltaic devices, an exciton diffusion length of 7 ± 1 nm has been deduced.[11] In this work, it was stressed that a precursor PPV with a relatively high glass transition temperature was used in order to avoid C_{60} interdiffusion into the relatively soft PPV layer. From photocurrent spectra on the same material combination, an exciton diffusion length of 12 ± 3 nm has been derived.[12] A more direct way, which decouples the device performance (photocurrent) from the exciton diffusion, is to study the quenching of the photoluminescence from polymer/fullerene bilayer heterostructures. The photogenerated exciton population is directly probed in this approach. The change of the photoluminescence with varying polymer layer thickness in a heterostructure directly reflects the change in exciton population due to their diffusion and subsequent charge transfer at the interface. The quenching of the photoluminescence (PL) of a ladder-type conjugated polymer, which was spin-coated on top of a [60]fullerene-derived self-assembled monolayer, has been measured, and an exciton diffusion length of 14 nm has been deduced from these measurements.[10] Furthermore, from the PL quenching of heterojunctions consisting of polythiophene and evaporated C_{60}, an exciton diffusion length of 5 nm has been obtained.[9]

A disadvantage of the precursor PPVs[11,12] is that they are not applicable in bulk heterojunction devices. In the present study, we investigate the exciton diffusion length in a random copolymer of poly(2-methoxy-5-(3′,7′-dimethyloctyloxy)-*p*-phenylene vinylene) and poly[4′-(3,7-dimethyloctyloxy)-1,1′-biphenylene-2,5-vinylene] (NRS−PPV, Figure 1a), which is a soluble PPV derivative. It is demonstrated that evaporation of C_{60} on top of these spin-coated layers results in ill-defined heterostructures. The C_{60} diffuses into the polymer layer on a time scale of several hours. As a result, analysis of the photoluminescence quenching of such a heterostructure leads to a strong overestimation of the exciton diffusion length. This problem can be

* Corresponding author. E-mail: D.Markov@rug.nl. Phone: +31 50 363 8336. Fax: +31 50 363 8751.
† Materials Science Centre^{Plus}, University of Groningen.
‡ Biomade Technology Foundation.

10.1021/jp0509663 CCC: $30.25
Published on Web 06/01/2005

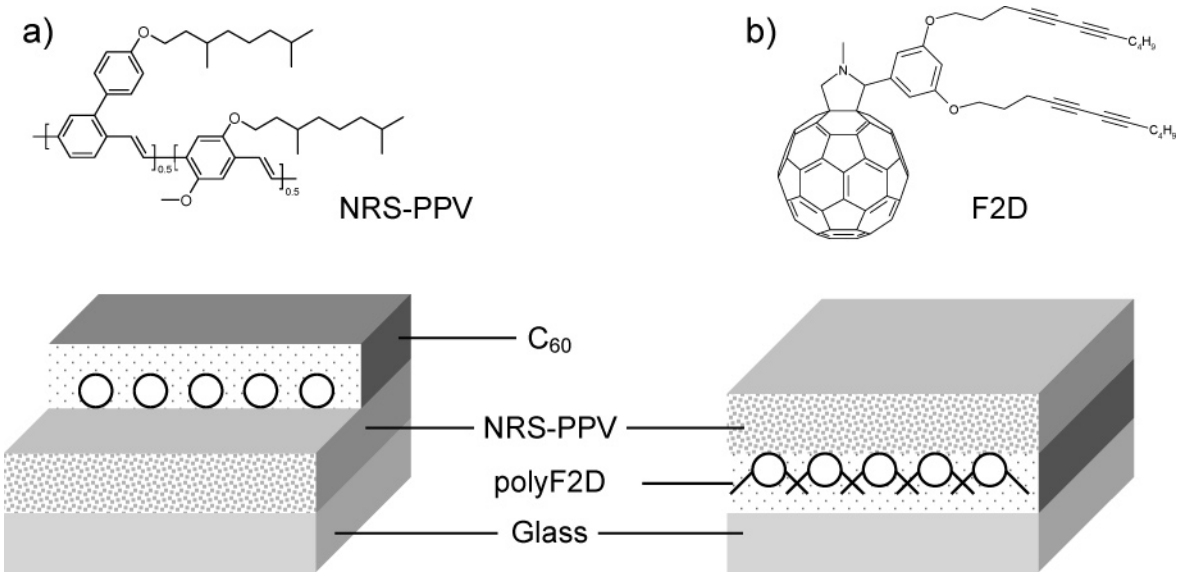

Figure 1. Schematic diagram of the sample configuration. C_{60} is evaporated on part of the polymer film (a). The poly(F2D) layer is formed by spin-coating and subsequent thermal polymerization/cross-linking of the F2D monomer layer. Subsequently, the NRS−PPV polymer is spun on top (b).

circumvented by the use of an immobilized acceptor layer. For this purpose, a new fullerene derivative with two diacetylene moieties is developed (F2D, see Figure 1b), which can be polymerized in the solid state. After polymerization, the resulting poly(F2D) layer is completely insoluble, and well-defined heterostructures can be constructed with any soluble material on top of it. Therefore, it serves as an ideal substrate acceptor material to study exciton diffusion in soft materials such as conjugated polymers. Photoluminescence quenching measurements on NRS−PPV/poly(F2D) heterostructures were performed, and an exciton diffusion length of 5 ± 1 nm was obtained. This is in agreement with earlier reported results,[11] where C_{60} in-diffusion was prevented as much as possible by choosing a "hard" precursor PPV.

2. Experimental Section

General. All diacetylenes, except F2D, were stored at −20 °C to minimize degradation. F2D was stored at room temperature in the dark. All chemicals are commercially available and were used as received. [60]Fullerene (99+%) was obtained from Bucky USA. ^{1}H and ^{13}C NMR spectroscopy were performed on a Varian VXR-300 (300 MHz) or a Varian Gemini-200 (200 MHz) instrument at 25 °C, using $CDCl_3$ as the solvent, unless stated otherwise. Values are reported in parts per million relative to trimethylsilane (TMS). Spectra recorded in CS_2 used D_2O (at 4.79 ppm relative to TMS) as an external lock. Multiplicities are denoted as follows: s = singlet, d = doublet, t = triplet, qn = quintet, m = multiplet; br means broad signal. Fourier transform (FT)-IR spectra were recorded on a Nicolet Nexus FT-IR spectrometer; solids were measured using a Smart Collector DRIFT setup; liquids were measured in transmission mode between NaCl windows. High-resolution mass spectrometry (HRMS) was performed on a JEOL JMS 600 spectrometer (EI, positive mode). High-performance liquid chromatography (HPLC) analyses of the fullerenes were performed on a Hewlett-Packard HP LC-Chemstation 3D (HP 1100 series) using an analytical Cosmosil Buckyprep column (4.6 mm × 250 mm). Mass spectra of the fullerene derivatives were obtained using an Agilent 1100 series LC/MSD coupled to this HPLC system.

Synthesis of 1-Bromo-1-hexyne.[13] In a large flask were placed 200 g of ice, 120 mL of a 10 M NaOH solution, 20 mL of bromine, and a solution of 16.4 g (0.20 mol) of 1-hexyne in 100 mL of tetrahydrofuran (THF). The resulting two-phase system was stirred vigorously for 96 h. To the resulting two-phase system was added 200 mL of saturated NH_4Cl solution, and the layers were separated. The aqueous layer was extracted three times with 100 mL of ether. The organic layers were combined, washed with 50 mL of brine, and dried over Na_2SO_4. The organic layer was concentrated in vacuo to approximately 50 mL. Distillation gave, after a forerun of residual THF and unreacted 1-hexyne, 19.6 g (0.122 mol, 61%) of 1-bromo-1-hexyne (bp 132−134 °C; lit. 35 °C at 12 mm Hg[14]) as a colorless liquid with a nasty smell, which rapidly turned yellowish upon exposure to light. It was stored in a brown bottle at −20 °C.

^{1}H NMR (200 MHz): δ 2.20 (t, 2H, J = 7.0 Hz), 1.56−1.34 (br m, 4 H), 0.90 (t, 3H, J = 7.0 Hz). ^{13}C NMR (50 MHz): δ 80.40, 37.39, 30.32, 21.85, 19.34, 13.53. IR (neat, cm^{-1}): 2959 (m), 2934 (m), 2873 (m), 2864 (m), 2219 (w), 1466 (w), 1070 (w), 744 (w).

Synthesis of Undeca-4,6-diyn-1-ol.[15] In a three-necked flask were placed 6.30 g (0.075 mol) of 4-pentyn-1-ol and 50 mL of pyrrolidine. The resulting solution was placed under nitrogen, and 1.43 g (7.5 mmol) of copper (I) iodide was added with stirring. Once this had dissolved, a solution of 15.1 g (0.094 mol) of 1-bromo-1-hexyne in 25 mL of pyrrolidine was added dropwise over 1 h with external cooling. The resulting mixture was stirred under N_2 at 20 °C for 3 h.

The red reaction mixture was poured onto 300 mL of saturated NH_4Cl solution (note: strongly exothermic!). The aqueous layer was extracted four times with 100 mL of ether. The organic layers were combined, washed with 50 mL of brine, and dried over Na_2SO_4. Evaporation of the solvents in vacuo gave 13.0 g of a dark red oil. Purification by column chromatography (silica gel; eluent petroleum ether (40−60 °C)/ethyl acetate = 2:1 (v/v)) gave 9.87 g (0.060 mol, 80%) of undeca-4,6-diyn-1-ol as a light-sensitive, yellowish oil.

^{1}H NMR (300 MHz): δ 3.74 (t, 2H, J = 6.2 Hz), 2.38 (t, 2H, J = 7.0 Hz), 2.25 (t, 2H, J = 7.0 Hz), 1.77 (qn, 2H, J = 6.6 Hz), 1.55−1.34 (br m, 5H), 0.90 (t, 3H, J = 7.1 Hz). ^{13}C NMR (75 MHz): δ 77.84, 76.36, 65.77, 65.02, 61.41, 30.95, 30.29, 21.87, 18.82, 15.71, 13.47. IR (neat, cm^{-1}): 3335 (s,

br), 2957 (s), 2934 (s), 2872 (s), 2257 (w), 2174 (w), 1467 (m), 1428 (m), 1056 (s). MS: *m/z* (relative intensity) 77 (66.5); 79 (60.1); 91 (100); 105 (33.4); 117 (26.7); 121 (26.2); 131 (16.8); 135 (14.7); 164 (22.5); 165 (2.8). Exact mass: Calcd for $C_{11}H_{16}O$ 164.1201. Found 164.1216.

Toluene-4-sulfonic Acid Undeca-4,6-diynyl Ester. To a solution of 2.0 g (12 mmol) of undeca-4,6-diyn-1-ol in 40 mL of dry pyridine at 0 °C were added four portions of 1.16 g (4 × 6.1 mmol) of tosyl chloride over a period of 10 min. The resulting mixture was stirred at 0 °C for 2 h and subsequently stored at 4 °C overnight.

The reaction mixture was poured onto 200 mL of ice/water, and 40 mL of concentrated hydrochloric acid was added. The aqueous layer was extracted four times with 100 mL of ethyl acetate. The organic layers were combined, washed with brine (50 mL), and dried over Na_2SO_4. Evaporation of the solvents gave 3.57 g of a dark oil. Purification by column chromatography (silica gel, eluent petroleum ether (40−60 °C)/ethyl acetate = 85:15 (v/v)) gave 2.89 g (9.1 mmol, 75%) of toluene-4-sulfonic acid undeca-4,6-diynyl ester as a colorless, light-sensitive oil.

^{1}H NMR (200 MHz): δ 7.78 (d, 2H, J = 8.3 Hz), 7.35 (d, 2H, J = 8.1 Hz), 4.11 (t, 2H, J = 6.0 Hz), 2.45 (s, 3H), 2.34−2.20 (m, 4H), 1.83 (qn, 2H, J = 6.5 Hz), 1.57−1.30 (m, 4H), 0.90 (t, 3H, J = 7.1 Hz). ^{13}C NMR (50 MHz): δ 144.80, 132.71, 129.86, 127.84, 78.06, 74.57, 68.61, 66.37, 64.86, 30.23, 27.61, 21.85, 21.61, 18.78, 15.44, 13.47. IR (neat, cm^{-1}): 2959 (m), 2933 (m), 2873 (w), 2257 (w), 1598 (w), 1363 (s), 1189 (s), 1176 (s), 930 (m). MS: *m/z* (relative intensity) 91 (89.3); 131 (70.6); 146 (100); 163 (66.7); 212 (2.2); 276 (2.0); 278 (1.1); 318 (1.2). Exact mass: Calcd for $C_{18}H_{22}O_3S$ 318.13. Not measured due to very low intensity of M^+ peak. MS (CI+): *m/z* 336.2 $(M + NH_4)^+$.

Synthesis of 3,5-Bis(undeca-4,6-diynyloxy)benzaldehyde. A mixture of 552 mg (4.0 mmol) of 3,5-dihydroxybenzaldehyde, 2.54 g (8.0 mmol) of toluene-4-sulfonic acid undeca-4,6-diynyl ester, 1.20 g (8.0 mmol) of NaI, and 1.40 g (10 mmol) K_2CO_3 in 25 mL of *N*,*N*-dimethylformamide (DMF) was stirred in the dark under N_2 at 55 °C for 48 h. The reaction mixture was poured onto 100 mL of ice/water, and the aqueous layer was extracted three times with ethyl acetate (50 mL). The organic layers were combined, washed subsequently with a saturated bicarbonate solution (50 mL) and with brine (25 mL), and dried over Na_2SO_4. Evaporation of the solvent in vacuo gave 1.96 g of crude product. Purification by column chromatography (silica gel, eluent petroleum ether (40−60 °C)/ether = 5:1 (v/v)) gave 0.93 g (2.2 mmol, 55%) of 3,5-bis(undeca-4,6-diynyloxy)-benzaldehyde as a yellowish, light-sensitive, waxlike solid, with a purity of >95% as determined by ^{1}H NMR.

^{1}H NMR (300 MHz): δ 9.89 (br s, 1H), 6.99 (s, 2H), 6.70 (s, 1H), 4.08 (t, 4H, J = 5.8 Hz), 2.48 (t, 4H, J = 6.6 Hz), 2.25 (t, 4H, J = 6.6 Hz), 2.00 (tt, appears as qn, 4H, J = 6.4 Hz (2×)), 1.54−1.34 (m, 8H), 0.90 (t, 6H, J = 7.1 Hz). ^{13}C NMR (75 MHz): δ 191.88, 160.39, 138.31, 108.02, 107.78, 78.01, 75.75, 66.52, 66.09, 65.00, 30.27, 27.94, 21.87, 18.83, 15.95, 13.49. IR (KBr, cm^{-1}): 3086 (w), 2957 (s), 2934 (s), 2872 (s), 2724 (w), 2257 (w), 2172 (w), 2147 (w), 1700 (s), 1605 (s), 1594 (s), 1454 (m), 1383 (m), 1296 (s), 1170 (s), 1062 (s). MS: *m/z* (relative intensity) 91 (66.2); 344 (37.7); 345 (12.5); 400 (38.7); 402 (15.9); 430 (100); 431 (32.7). Exact mass: Calcd for $C_{29}H_{34}O_3$ 430.2503. Found 430.2508.

Synthesis of 1′-Methyl-1′,5′-dihydro-2′-(3,5-bis(undeca-4,6-diynyloxy)phenyl)-*1H*-pyrrolo[3′,4′:1,9](C$_{60}$-*I$_h$*)[5,6]fullerene (F2D). A mixture of 720 mg (1.0 mmol) of C_{60}, 432 mg (1.0 mmol) of 3,5-bis(undeca-4,6-diynyloxy)benzaldehyde (>95% pure), and 270 mg (3.0 mmol) of sarcosine in 100 mL of *o*-dichlorobenzene was heated under N_2 at 85 °C for 20 h. The reaction mixture was concentrated in vacuo to ∼15 mL, and the product was isolated by column chromatography (silica gel; toluene). Unreacted C_{60} was removed using CS_2 (recovered: 270 mg), and subsequently, the monoadduct was isolated using toluene/cyclohexane = 2:1 (v/v). The product was redissolved in 10 mL of chlorobenzene, precipitated with MeOH, washed repeatedly with MeOH and pentane, and dried in vacuo at 55 °C. This gave 367 mg (0.31 mmol, 31%) of F2D.

^{1}H NMR (300 MHz, CS_2/D_2O): δ 7.12 (br s, 2H), 6.57 (t, 1H, J = 2.0 Hz), 5.19 (d, 1H, J = 9.2 Hz), 5.07 (s, 1H), 4.50 (d, 1H, J = 9.2 Hz), 4.24 (t, 4H, J = 5.9 Hz), 3.09 (s, 3H), 2.67 (t, 4H, J = 6.6 Hz), 2.48 (t, 4H, J = 6.5 Hz), 2.19 (tt, appears as qn, 4H, J = 6.4 Hz (2×)), 1.80−1.62 (m, 8H), 1.21 (t, 6H, J = 7.0 Hz). ^{13}C NMR (75 MHz, CS_2/D_2O): δ 159.8 (br), 155.79, 153.69, 153.22, 153.11, 147.04, 147.02, 146.70, 146.16, 146.08, 145.98, 145.90, 145.87, 145.84, 145.77, 145.69, 145.56, 145.39, 145.26, 145.17, 145.13, 145.05, 145.00, 144.92, 144.53, 144.46, 144.17, 144.12, 142.89, 142.76, 142.46, 142.34, 142.05, 141.99, 141.92, 141.86, 141.81, 141.66, 141.45, 140.01, 139.93, 139.64, 139.51, 138.82, 136.45, 136.19, 135.55, 110−106 (br), 101.55, 83.27, 77.56, 76.69, 75.85, 69.79, 68.68, 67.51, 66.73, 65.93, 39.87, 30.76, 28.54, 22.46, 19.29, 16.36, 13.99. IR (KBr, cm^{-1}): 2952 (s), 2932 (s), 2870 (m), 2834 (m), 2779 (s), 2327 (w), 2258 (w), 2196 (w), 2086 (w), 1594 (s), 1462 (s), 1450 (s), 1162 (s), 1062 (m), 527 (s). MS: *m/z* 720.0; 1177.2 (M−). Calcd for $C_{91}H_{39}NO_2$: 1177.3.

Synthesis of 3,5-Didodecyloxybenzaldehyde. A mixture of 280 mg (2.0 mmol) of 3,5-dihydroxybenzaldehyde, 1.05 g (4.2 mmol) of dodecyl bromide, 0.70 g (5.0 mmol) of K_2CO_3, 10 mg of NaI, and 15 mL of DMF was stirred at 60 °C for 3 days. The reaction mixture was cooled to room temperature and mixed with 100 mL of ice/water. The resulting aqueous layer was extracted with ethyl acetate (1 × 100 mL, 2 × 50 mL). The organic layers were combined, washed subsequently with 25 mL of saturated $NaHCO_3$ solution and with 25 mL of brine, and dried over Na_2SO_4. Evaporation of the solvent in vacuo gave 1.44 g of crude product. Purification by column chromatography (silica gel, eluent petroleum ether (40−60 °C)/ether = 19:1 (v/v)) gave 0.89 g (1.9 mmol, 94%) of product as a white solid.

^{1}H NMR (200 MHz): δ 9.89 (s, 1H), 6.98 (d, 2H, J = 2.2 Hz), 6.70 (d, 1H, J = 2.2 Hz), 3.98 (t, 4H, J = 6.5 Hz), 1.85−1.72 (m, 4H), 1.44−1.21 (m, 36H), 0.88 (t, 6H, J = 6.4 Hz). ^{13}C NMR (50 MHz): δ 192.08, 160.75, 138.29, 107.99, 107.57, 68.42, 31.91, 29.63, 29.57, 29.34, 29.11, 25.99, 22.68, 14.11. IR (KBr, cm^{-1}): 3093 (w), 2955 (m), 2918 (s), 2848 (s), 2725 (w), 1687 (s), 1597 (s), 1467 (m), 1386 (m), 1294 (m), 1181 (s), 1067 (s). MS: *m/z* (relative intensity) 138 (27.1); 139 (12.7); 306 (19.0); 474 (100); 475 (34.2). Exact mass: Calcd for $C_{31}H_{54}O_3$ 474.4073. Found 474.4074.

Synthesis of 1′-Methyl-1′,5′-dihydro-2′-(3,5-didodecyloxyphenyl)-*1H*-pyrrolo[3′,4′:1,9](C$_{60}$-*I$_h$*)[5,6]fullerene (F2C12). A mixture of 475 mg (1.0 mmol) of 3,5-didodecyloxybenzaldehyde, 300 mg (3.1 mmol) of sarcosine, and 1.08 g (1.5 mmol) of C_{60} in 100 mL of chlorobenzene was heated under N_2 at 95 °C overnight. The brown solution was cooled to room temperature and concentrated in vacuo. The resulting solid was dissolved in *o*-dichlorobenzene (ODCB) (20 mL), and the product was isolated by column chromatography as described for F2D. The monoadduct was dissolved in 20 mL of toluene,

precipitated with methanol, and washed as described for F2D. Yield: 480 mg (0.43 mmol, 43%) of F2C12 as brown powder.

^{1}H NMR (300 MHz, CS_2/D_2O): δ 7.2−6.9 (br s, 1H), 6.51 (s, 1H), 5.20 (d, 1H, J = 9.2 Hz), 5.05 (s, 1H), 5.50 (d, 1H, J = 9.2 Hz), 4.13 (t, 4H, J = 6.0 Hz), 3.16 (s, 3H), 2.04−1.95 (m, 4H), 1.71−1.48 (m, 36H), 1.18 (t, 6H, J = 6.4 Hz). ^{13}C NMR (300 MHz, CS_2/D_2O): δ 160.1 (br), 155.83, 153.73, 153.36, 153.19, 147.04, 147.01, 146.76, 146.17, 146.08, 145.99, 145.92, 145.87, 145.83, 145.70, 145.52, 145.39, 145.36, 145.27, 145.20, 145.15, 144.99, 144.91, 144.47, 144.15, 144.14, 142.93, 142.78, 142.46, 142.38, 142.03, 142.00, 141.93, 141.90, 141.84, 141.69, 141.64, 141.45, 141.41, 140.02, 139.92, 139.62, 139.48, 138.50, 136.45, 136.15, 135.54, 110−105 (br), 101.44, 83.37, 76.70, 69.78, 68.69, 67.64, 39.88, 32.27, 30.07, 30.03, 29.84, 29.75, 29.61, 26.46, 23.27, 14.60. IR (KBr, cm^{-1}): 2923 (s), 2852 (s), 2779 (s), 2327 (w), 2196 (w), 2131 (w), 2085 (w), 1595 (m), 1462 (m), 1162 (m), 1059 (m), 527 (s). MS: *m*/*z* 720.0; 1221.4 (M−). Calcd for $C_{93}H_{59}NO_2$: 1221.4.

Polymerization of F2D. Films of F2D were drop-cast from chloroform solutions onto glass slides. Subsequently, the resulting films were allowed to dry, and then, the slides were transferred into a glovebox for polymerization experiments. Heating experiments were performed with the glass slides on a hotplate. The temperatures reported are those set for the hotplate, since this was found to be the most reproducible value. Attempts were made to determine the actual temperatures on top of the glass slides using a contact thermometer, and they were found to be somewhat varying; we estimate them as roughly 15−20 °C lower than those set as temperature for the hotplate. After heating, the films were tested for their (in)solubility in ODCB, which is a very good fullerene solvent, to test for successful polymerization and cross-linking. The glass slides were broken into small pieces and placed in a test tube. Subsequently, 1 mL of ODCB was added, and the tubes were closed and allowed to stand in the dark for 24 h. If after this time the solution did not get a color, the film was considered insoluble. Those films were put aside for another 24 h in ODCB to verify the insolubility. Final tests for insolubility of the films were done by taking a small drop of the ODCB solution, allowing this to dry on a thin-layer chromatgraphy (TLC) silica gel plate, and checking if a colorless spot was obtained.

Exciton Diffusion Length Measurements. *A. Sample Preparation.* In Figure 1, an overview is given of the typical sample configuration and the materials used in this study. Two types of donor−acceptor bilayer systems were fabricated on top of glass substrates. In the first structure, thin films of NRS−PPV were deposited by spin-casting from a toluene solution in nitrogen atmosphere. A series of NRS−PPV layer thicknesses ranging from 4 to 165 nm were obtained by varying the polymer solution concentration and spin frequency. Subsequently, glass/NRS−PPV/C_{60} structures were prepared by evaporation of C_{60} on top of the polymer film under high vacuum ($P < 3 \times 10^{-7}$ mBar) with an evaporation rate of about 0.05 nm/s. In the second structure, the fulleropyrrolidine monomer (F2D, Figure 1b) was spin-coated from a chlorobenzene solution on top of the glass substrate to yield a 40 nm thick layer. Full thermopolymerization of the fullerene layer was achieved during 20 min at 250 °C to obtain a completely insoluble film of poly(F2D). Subsequently, NRS−PPV in a toluene solution was spin-coated on top. The film thicknesses and surface roughness were characterized by a surface profilometer (Dektak 6M), by optical absorption spectroscopy, and by atomic force microscopy.

B. Optical Techniques. The quenching of the luminescence can be monitored by either measuring the change of the luminescence decay using time-resolved measurements or by measuring the absolute steady-state luminescence output using an integrating sphere. The advantage of the first approach is that it is less sensitive to slight variations in the experimental conditions, since the decay curve can be normalized to its maximum value. Time-resolved optical experiments were carried out with the output of a mode-locked femtosecond Ti:sapphire laser. Laser pulses were frequency-doubled, and PPV excitation was performed at 400 nm, with p-polarized light at 64° incident angle in order to minimize internal reflections. Typical time-averaged excitation intensities on the sample were about 30 mW/cm^2. Emission was collected normal to the excitation beam. To avoid degradation, samples were sealed under nitrogen in a cell with a quartz window. In time-correlated single photon counting (TCSPC) experiments,[16] an instrument response function of 30 ps (full width at half-maximum) was used for the deconvolution of the luminescence decay. For consistency, luminescence quenching for the same samples of NRS−PPV polymer layers partly covered with C_{60} was also obtained by steady-state measurements, using an integrating sphere (Labsphere) with argon-ion laser (Spectra-physics) excitation at 458 nm. The results of the time-resolved data were found to be identical to the results obtained from these steady-state measurements in the test samples used for this comparison. In this study, the time-resolved data are presented to analyze the luminescence quenching and exciton diffusion experiments over the whole range of thicknesses measured. All optical experiments were performed at room temperature.

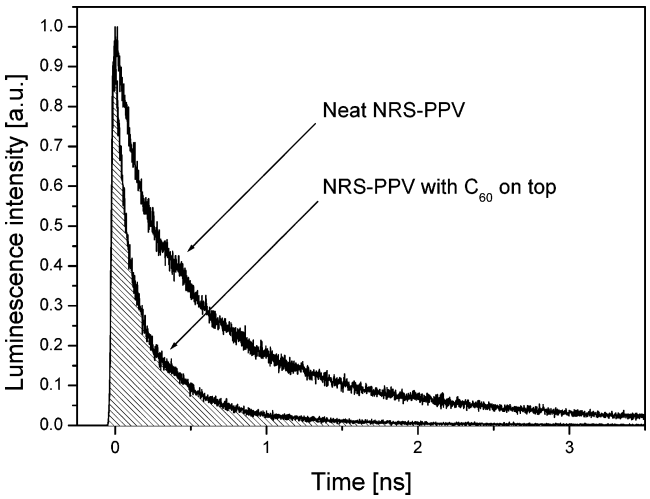

Figure 2. Normalized photoluminescence decay of 30 nm NRS−PPV film with and without evaporated C_{60} on top, measured at the emission maximum of 580 nm.

3. Results and Discussion

PPV/C60 Structures. In Figure 2, the normalized photoluminescence decay curves, as obtained by TCSPC measurements, of a 30 nm NRS−PPV film with and without evaporated C_{60} on top are shown. The devices were excited from the PPV side at a wavelength of 400 nm, and the emission was collected at 580 nm, which corresponds to the maximum of the luminescence spectrum. The PL of the sample covered with C_{60} obviously decays faster, because of the luminescence quenching by efficient electron transfer from the PPV donor to the C_{60} acceptor.

To simulate the quenching of the excited states in the polymer layer, the following one-dimensional continuity equation for the photoexcitation density[9,10] $n(x, t)$ is used

$$[\partial n(x, t)/\partial t] = -[n(x, t)/\tau_0] + D[\partial^2 n(x, t)/\partial^2 x] - S(x)n(x, t) + g(x, t) \quad (1)$$

The spatial variable x represents the distance from the glass/polymer interface. The first term on the right-hand side of eq 1 accounts for the process of radiative and nonradiative decay of the excited states in the neat polymer film, characterized by a single-exponential decay time constant τ_0. The second term is the one-dimensional exciton diffusion characterized by the diffusion coefficient D. The dissociation of photoexcitations via electron transfer at the polymer/fullerene interface is represented by the third term. The last term describes the exciton generation process and is governed by the spatially dependent intensity of the femtosecond laser pulse.

The characteristic distance of exciton diffusion in one dimension is the exciton diffusion length, defined as

$$L_D = \sqrt{D\tau_0} \quad (2)$$

For the further model construction, we assume an infinite exciton quenching rate at the polymer/fullerene interface. This implies an exciton diffusion-limited luminescence quenching in polymer/fullerene heterostructures. Two decades ago, it had been extensively demonstrated that a similar model, applied in molecular crystals with exciton traps, can cause a dramatic underestimation of the characteristic diffusion parameters: diffusion constant D and diffusion length L_D.[17] This originates from the fact that two distinct rates govern the total exciton quenching process: the rate at which excitons migrate into the regions occupied by trap molecules, quantified by the diffusion term in eq 1, and second, the rate at which an excitation decays to the trap states from neighboring host molecules once it approaches a trap, described by the dissociation (capture) term in eq 1 given by $-S(x)n(x, t)$. Thus, luminescence quenching by exciton traps introduced into *organic crystals* has been proven to be capture- but not motion-limited, which results from the fact that the exciton motion is faster then the exciton capture by traps. In this paper, we consider the slow (activated) exciton diffusion in *highly disordered* conjugated polymers, driven by a hopping mechanism between long chain segments.[18] This slow diffusion occurs after picosecond exciton relaxation within an inhomogeneously broadened density of states (DOS).[19] The dwell time of an excitation in PPV is estimated to be on the order of ~3 ps.[20] In contrast, a short-range exciton capture by the efficient electron transfer from the conjugated polymer to the fullerene[21] occurs with a characteristic time of 45 fs.[22] Therefore, the dwell time between consequent hopping steps in the investigated diffusion process in conjugated polymer is much longer then the exciton quenching time at the polymer/fullerene interface. Unlike in organic crystals, this strongly suggests that the exciton quenching in conjugated polymer/fullerene heterostructures is truly diffusion-limited. As a helpful method to discriminate between capture and motion effects, surface-quenched time-resolved luminescence experiments have been also suggested.[17,23] Recent time-resolved luminescence decay measurements in conjugated polymer/fullerene heterostructures confirmed the dominance of diffusion-limited exciton quenching.[24]

Consequently, eq 1 can be simplified by assuming an infinite exciton quenching rate at the polymer/fullerene interface, without any x dependence. As a result, the term responsible for surface quenching can be removed, and for a polymer film with thickness L, the boundary condition $n(x = L) = 0$ at the polymer/fullerene interface is used. At the interfaces with no fullerene present (i.e., the polymer/nitrogen and substrate/polymer interfaces), we use the boundary condition $\partial n/\partial x = 0$ assuming low surface quenching.[9]

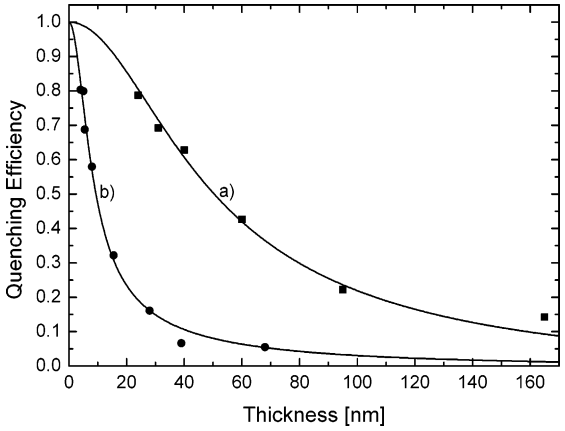

Figure 3. The relative luminescence quenching in polymer/C_{60} (a) and polymer/poly(F2D) (b) heterostructures for different polymer film thicknesses. Fits of these data with eq 3 (solid lines) using exciton diffusion lengths of 28 and 5 nm for (a) and (b), respectively, are shown.

The relative quenching efficiency Q is defined as 1 minus the number of photons emitted from the polymer film with C_{60} evaporated on top, normalized to the number of emitted photons from the neat polymer film with equal thickness

$$Q(L, L_D) = 1 - \frac{\int_0^\infty \int_0^L n_{\text{pol/fullerene}}(x, t, L_D)\, dx\, dt}{\int_0^\infty \int_0^L n_{\text{neat.pol.}}(x, t, L_D)\, dx\, dt} \quad (3)$$

The integrals in eq 3 represent the total time-integrated photoluminescence of the polymer films with and without the C_{60} layer, respectively. Consequently, Q is a function of the polymer film thickness L as well as the exciton diffusion length L_D. To quantify the luminescence quenching efficiency from the time-resolved data, the luminescence decay curves for the samples with different polymer thicknesses were normalized, and the areas under the curves were determined, representing the time-integrated emission (Figure 2). Upon reduction of the polymer film thickness, a larger portion of the excited states will reach the polymer/C_{60} interface. As a result, the relative quenching efficiency will increase, as is represented in Figure 3a.

To obtain the exciton diffusion length, eq 3 has to be fitted to the luminescence quenching efficiency data, with the photoexcitation density $n(x, t, L_D)$ governed by eq 1. The time-integrated approach, used to obtain the quenching efficiency Q, is equivalent to steady-state quenching, and the exciton density distribution time derivative in eq 1 can be set to zero. Then, the exciton quenching yield Q as a function of polymer film thickness L is given by

$$Q = \frac{[a^2 L_D{}^2 + aL_D \tanh(L/L_D)] \exp(-aL) - a^2 L_D{}^2 [\cosh(L/L_D)]^{-1}}{(1 - a^2 L_D{}^2)[1 - \exp(-aL)]} \quad (4)$$

with a as the absorption coefficient and L_D the exciton diffusion length as defined above eq 2, being the only fit parameter in this model. The best fit (Figure 3a, solid line) is obtained for a diffusion length of 28 nm in the NRS−PPV/C_{60} sample. This value is several times higher than all other values reported in the literature for conjugated polymers (7−14 nm).[9−12] A possible

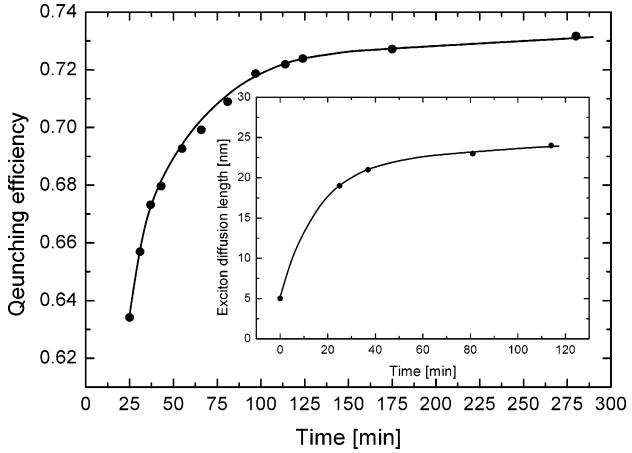

Figure 4. Growth of the relative quenching for the 26 nm polymer film with evaporated C_{60} on top in time. The C_{60} evaporation starts at $t = 0$. The inset shows the increase of the apparent exciton diffusion distance as a function of time.

explanation for this very long quenching length could be the intermixing of the evaporated C_{60} molecules with the soft polymer layer, which would obscure the intrinsic exciton diffusion process. From photoelectron spectroscopy and X-ray absorption, it has been demonstrated that C_{60} diffuses at room temperature into a spin-coated poly(3-octylthiophene) (P3OT) layer after deposition by evaporation.[25] The time scale of this in-diffusion process of C_{60} into P3OT typically amounts to $^1/_2$ h. With this in mind, we followed the time dependence of the luminescence quenching efficiency for an NRS−PPV film after evaporation of a C_{60} film (Figure 4). The time required to vent the evaporator, take out the devices, mount them in the optical setup, and perform the first time-resolved PL scans was typically 20−25 min. After this period, it is clearly observed from Figure 4 that the luminescence quenching yield of the 26 nm NRS−PPV layer is still increasing in time, indicative of a slow C_{60} diffusion into the polymer film. After typically 2 h, the quenching length approaches its maximum value of 28 nm as shown in the inset of Figure 4, which gives an indication about the C_{60} diffusion rate at room temperature. From the measured quenching lengths and corresponding time dependence, it is clear that evaporation of C_{60} on top of spin-coated conjugated polymers leads to ill-defined heterojunctions. Therefore, in these devices, it is not possible to obtain information about the intrinsic exciton diffusion process in NRS−PPV.

Side-Chain Cross-Linked Fullerene/PPV Heterojunctions. One solution to measure the intrinsic values of exciton diffusion is to choose a polymer with a high glass transition temperature[11] as a precursor PPV, to prevent C_{60} interdiffusion as much as possible. A disadvantage of this approach is that it is not applicable to the soluble polymers that are used in photovoltaic devices, on the basis of blends of PPV and fullerenes. In this study, an alternative approach is presented: Instead of an evaporated C_{60} layer as an acceptor, we use a side-chain cross-linked fullerene layer.

Thermal polymerization and cross-linking are preferred for this fullerene layer, because light-induced polymerization can be complicated because of the absorption of a large portion of the light by the fullerene, thus reducing the desired side-chain reactivity of the monomer and opening pathways for fullerene-related photochemical reactions. A possible thermally polymerizable system is a fullerene derivative containing two or more diacetylene groups. Diacetylenes can be thermally polymerized, and this reaction is rapid,[26] which is convenient from a practical point of view. Preferably, the process should take place in the solid state, to prevent, for example, dewetting of the substrates or mixing of the molten fullerene layer with an underlying organic layer, if such a layer is present.

Hirsch and co-workers have already reported a system comparable to that discussed above.[27,28] They demonstrated photochemical polymerization of a so-called hexakis Bingel adduct containing 12 diacetylene groups. However, there are a few drawbacks to the use of their system. A large number of diacetylene-functionalized alkyl chains per fullerene unit were needed to obtain insoluble films.[28] Hexakis adducts of C_{60} are expected to be far less effective as the quenching layer materials (compared to monoadducts) in our photoluminescence quenching experiments. Also, the reaction reportedly took several days, and it occurred in the liquid state. As mentioned above, this is not ideal, and therefore, an improved system was developed, which can be polymerized in the solid state.

The structure and synthesis of the polymerizable fullerene derivative F2D that was used in this study are shown in Figure 1b and Figure I, respectively. F2D is a so-called Prato adduct and contains two diacetylene groups, because at least two such groups per fullerene unit are required to obtain both polymerization and three-dimensional cross-linking. This cross-linking is necessary in order to obtain a really insoluble fullerene film from the processable monomer. The presence of more than two

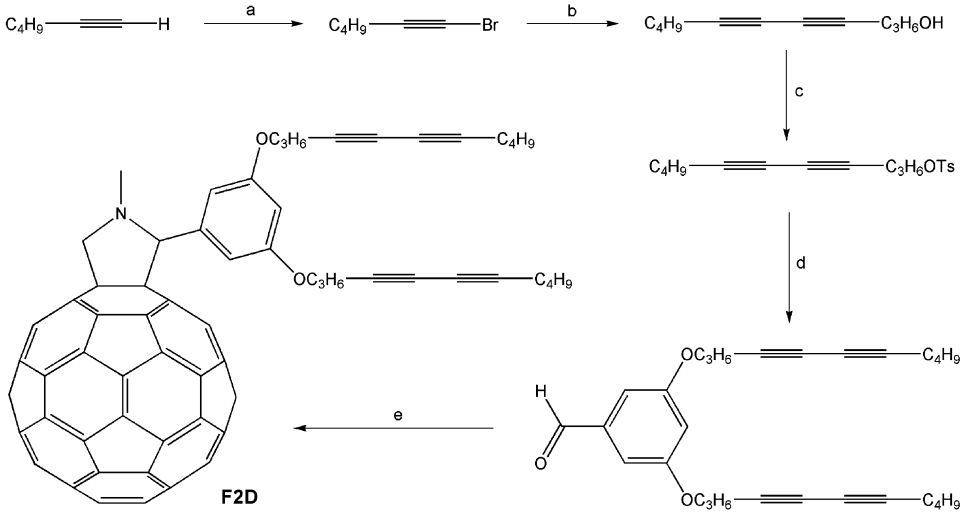

Figure 5. Synthesis of F2D. (a) NaOH, Br_2, H_2O/THF, 96 h, 61%. (b) 4-pentyn-1-ol, CuI, C_4H_9N, 3 h, 80%. (c) TsCl, C_5H_5N, 0 °C, 20 h, 75%. (d) 3,5-dihydroxybenzaldehyde (0.5 equiv), K_2CO_3, NaI, DMF, 55 °C, 48 h, 55%. (e) C_{60}, $NH(CH_3)CH_2COOH$, C_6H_5Cl, 85 °C, 20 h, 31%.

diacetylene groups would in theory be superfluous. Relatively short alkoxy spacers containing only three methylene groups are present between the diacetylene moieties and the aryl group that links them to the fulleropyrrolidine. This structure was chosen, because the reactive groups have a reasonable amount of flexibility, while at the same time, the amount of inactive material (i.e., alkyl groups) is kept at a minimum, which is relevant if such derivatives are to be used for (opto)electronic applications. The butyl end groups approximately match the length of the propyloxy spacers, thus allowing for possible interdigitated structures. Besides, 1-bromo-1-alkynes smaller than 1-bromo-1-hexyne are inconvenient from a synthetic point of view.[14]

The appropriate diacetylene-containing alkyl chains were prepared by a selective cross-coupling of 4-pentynol with 1-bromo-1-hexyne, using an excess of the latter. This is in contrast to the original procedure,[15] where the best results were obtained using an excess of the acetylenic alcohol. However, in our experiments, it was found that in that case the product after chromatography always contained a residual amount of this alcohol, which was difficult to remove completely[29] and would give side products in subsequent steps. Thus, the modified procedure was preferred. The alcohol group was converted into the tosylate, and the resulting compound was then coupled with 3,5-dihydroxybenzaldehyde. Finally, a Prato reaction[30] of this benzaldehyde derivative with C_{60} gave the desired fulleropyrrolidine (F2D).

The structure of compound F2D was confirmed by ^{1}H and ^{13}C NMR and IR spectroscopy, as well as by mass spectrometry. Interestingly, the ortho C atoms of the aryl group seemed to be missing in the ^{13}C NMR spectrum. However, they showed up as a broad peak with low intensity. This is most likely the result of the severely hindered rotation of the phenyl group due to the presence of the two long alkyl chains at the meta positions, which will have to move a long distance through the solvent when the aryl ring rotates.[31] As a result, in addition, the signals from the other aromatic carbons atoms were broadened in the ^{13}C NMR spectrum.

To investigate the thermal polymerization of F2D, films were drop-cast on glass slides and heated in a nitrogen atmosphere on a hotplate at various temperatures for a certain time (usually 0.5, 1, 2, and 3 h). Subsequently, the heated films were tested for their (in)solubility by immersing them in ODCB in a closed test tube for 24 h. These experiments revealed that there was a threshold temperature for polymerization. Below 150 °C, the monomer did not react at all, even after heating for several hours. At around 175 °C, a reaction took place, and films that were virtually insoluble in ODCB were obtained after 2−3 h of heating. At still higher temperatures (≥200 °C), the product films became completely insoluble within 30 min of heating. In a series of control experiments, a fulleropyrrolidine bearing two dodecyl groups instead of the two diacetylene-containing alkyl chains (F2C12, see Figure 6) showed no reactivity or instability up to at least 250 °C. Heated films of F2C12 always dissolved almost instantly in ODCB after the thermal "annealing" step, and analysis showed only pure monomer. Thus, it was concluded that the formation of the insoluble films must be the result of cross-linking of the diacetylene groups in the film, not of reactions or degradation of the fullerene moiety.

Insoluble films of organic compounds are not easily analyzed in great detail. In this particular case, it is presumed (and desired) that the major part of the molecule (i.e., the fullerene) plays no role whatsoever in the polymerization process and will remain unchanged. This means that there will be only minor differences

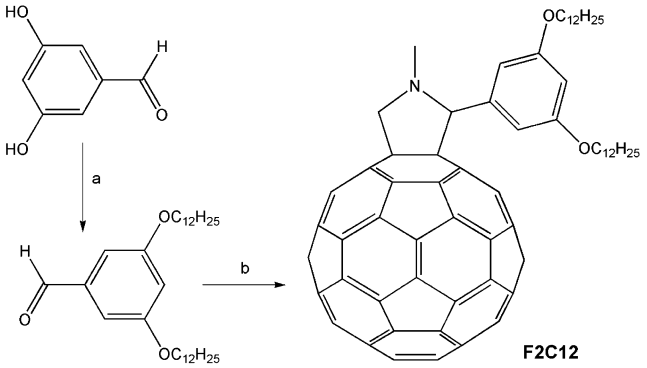

Figure 6. Synthesis of F2C12. (a) $C_{12}H_{25}Br$ (2 equiv), K_2CO_3, NaI, DMF, 60 °C, 72 h, 94%. (b) C_{60} (1.5 equiv), $NH(CH_3)CH_2COOH$, C_6H_5-Cl, 95 °C, 20 h, 43%.

in the overall chemical structure of the films before and after, which is a drawback for their analysis. The fullerene derivatives contain mainly sp^2 and sp^3 carbon atoms, which rules out techniques such as XPS, as the disappearance (actually only a decrease) of the small number of sp hybridized carbon atoms will be difficult to detect. UV−vis spectroscopy seems a possibility, but for an accurate comparison of the films before and after polymerization, exact repositioning of the substrate after heating is required to eliminate the effects of differences in reflection and/or diffraction of the light. An attempt was made using spin-cast films on quartz slides, but the spectrum after heating showed no new peaks compared to that of untreated F2D. The disappearance of the diacetylene moieties could not be seen, as this absorption is overshadowed by the strong absorptions of the fullerene moiety, and only some broadening in the region of the fullerene absorption was observed. This is most likely because the poly(enyne)s formed in the polymerization/cross-linking will all be of varying length and structure, thus giving rise to a broad, low-intensity absorption.

The reaction of the diacetylene groups was confirmed by IR spectroscopy. After polymerization, the films were scraped from the glass slides using KBr powder for sandpaper, and the resulting dispersions were investigated in diffuse reflection (DRIFT) experiments. In this way, the whole film is analyzed, not just the top layer. The results are shown in Figure 7.

The two spectra in Figure 7 are rather similar. The IR absorptions in the poly(F2D) spectrum have somewhat broadened compared to those of the monomer. All vibrations of those parts of the molecule that are not involved in the polymerization process are still present with their relative intensity virtually unchanged. The only clearly visible change is in the diacetylene vibration at 2258 cm^{-1}, which has disappeared (see inset), and a broad new vibration around 2220 cm^{-1} has appeared. These changes in the spectrum of the material before and after polymerization compare well to those reported in the literature for other polymerized diacetylenes,[32,33] indicating that poly(F2D) must have formed and that the reaction has proceeded in the desired manner. The vibrations of the C_{60} moiety seem not to have been affected by the polymerization (see inset). The pattern in the 600−500 cm^{-1} range is highly similar for F2D and poly(F2D). Thus, at least the major part of the fullerenes has not reacted and remains intact. This has been reported before, in a system where diacetylenes were polymerized in the presence of a C_{60} derivative.[34]

The poly(F2D) system discussed above is an ideal model system to study exciton diffusion in heterojunctions with any soluble conjugated polymers which are interesting for organic solar cells. After thermal polymerization/cross-linking, the

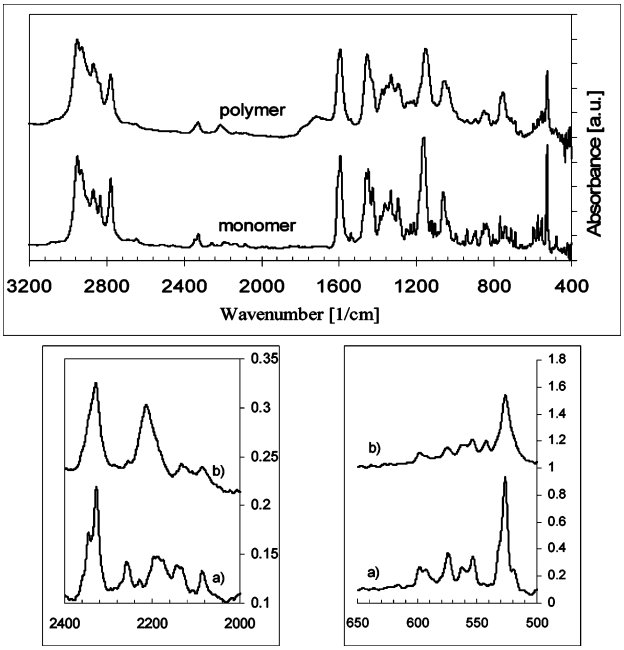

Figure 7. IR absorption spectra of F2D (a) and poly(F2D) (b). The insets show enlargements of the two areas that are discussed in the text.

fullerene molecules are immobilized, preventing them from diffusing into the polymer, and the poly(F2D) layer is totally insoluble, even in good fullerene solvents. Since the exciton diffusion length is expected to be on the order of 5−10 nm, it is important to characterize the surface roughness of the poly(F2D) films. F2D spin-cast and thermopolymerized/cross-linked film surface was characterized with atomic force microscopy, and the root-mean-square (RMS) of less than 0.8 nm was determined. Furthermore, we observed that the films are smooth and uniform without interfacial voids, which could mask the intrinsic exciton diffusion length. Consequently, the conjugated polymer can be spin-cast on top of the fullerene layer without any interdiffusion of the two materials taking place.

Glass/poly(F2D)/NRS−PPV samples with varying PPV film thicknesses were prepared by spin-coating NRS−PPV from toluene solution on top of the side-chain polymerized fullerene layer. Luminescence quenching measured on these samples was found to be stable in time, in contrast to the structures with evaporated C_{60} on the polymer, showing the absence of fullerene diffusion into the polymer film. The luminescence quenching observed for this sample structure is relatively small; the results are represented in Figure 3b. By attributing this quenching to the exciton diffusion toward a well-defined polymer/fullerene interface, the experimental data are fitted well by taking an exciton diffusion length of 5 ± 1 nm (Figure 3b, solid line). This value is significantly lower than the characteristic quenching range determined from the NRS−PPV/C_{60} heterostructure. The exciton diffusion length of 5 ± 1 nm that we estimated for NRS−PPV is in close agreement with the values found for the precursor PPV (7 ± 1 nm) that was determined by photovoltaic response simulation[11] and for polythiophene as obtained from luminescence quenching (5 nm).[9] Consequently, in polymer/fullerene photovoltaic devices, the dissociation of excitons is confined to a region of only a few nanometers from the donor/acceptor interface. Our results strongly suggest that the large range of exciton diffusion lengths reported in the literature is due to the interdiffusion of the donor and acceptor materials.

4. Summary and Conclusion

In conclusion, we have studied photoluminescence quenching in PPV/fullerene heterostructures by means of time-resolved luminescence measurements. It is demonstrated that C_{60} evaporated on top of a spin-coated PPV layer diffuses into the polymer, thereby masking the intrinsic exciton diffusion process. Well-defined PPV/fullerene heterojunctions are obtained by using a newly developed polymerizable fullerene layer, made by thermal side-chain polymerization/cross-linking at ≥200 °C of a fulleropyrrolidine derivative, F2D, that contains two diacetylene moieties. The fullerene layer is cross-linked by polymerization of those diacetylene groups. This has been confirmed by IR spectroscopy and by investigations on a reference compound without the reactive groups (F2C12) that did not react at all. Thus, after thermopolymerization, the acceptor molecules are immobilized, and a sharp heterojunction is obtained between the polymerized fullerene layer and a spin-coated NRS−PPV film. In this model system, an exciton diffusion length of 5 ± 1 nm was obtained.

Acknowledgment. This work is part of the research program of the Stichting voor Fundamenteel Onderzoek der Materie (FOM, financially supported by the Nederlandse Organisatie voor Wetenschappelijk Onderzoek (NWO)).

References and Notes

(1) Sariciftci, N. S. *Prog. Quantum Electron.* **1995**, *19*, 131.
(2) Halls, J. J. M.; Walsh, C. A.; Greenham, N. C.; Marseglia, E. A.; Friend, R. H.; Moratti, S. C.; Holmes, A. B. *Nature (London)* **1995**, *376*, 498.
(3) Brabec, C. J.; Sariciftci, N. S.; Hummelen, J. C. *Adv. Funct. Mater.* **2001**, *11*, 15.
(4) Shaheen, S. E.; Brabec, C. J.; Sariciftci, N. S.; Padinger, F.; Fromherz, T.; Hummelen, J. C. *Appl. Phys. Lett.* **2001**, *78*, 841.
(5) Wienk, M. M.; Kroon, J. M.; Verhees, W. J. H.; Knol, J.; Hummelen, J. C.; van Hal, P. A.; Janssen, R. A. J. *Angew. Chem., Int. Ed.* **2003**, *42*, 3371.
(6) Hoppe, H.; Arnold, N.; Sariciftci, N. S.; Meissner, D. *Sol. Energy Mater. Sol. Cells* **2003**, *80*, 105.
(7) van Duren, J. K. J.; Yang, X.; Loos, J.; Bulle-Lieuwma, C. W. T.; Sieval A. B.; Hummelen, J. C.; Janssen, R. A. J. *Adv. Funct. Mater.* **2004**, *14*, 425.
(8) Sariciftci, N. S.; Heeger, A. J. *Int. J. Mod. Phys. B* **1994**, *8*, 237.
(9) Theander, M.; Yartsev, A.; Zigmantas, D.; Sundstrom, V.; Mammo, W.; Andersson, M. R.; Inganas, O. *Phys. Rev. B* **2000**, *61*, 12957.
(10) Haugeneder, A.; Neges, M.; Kallinger, C.; Spirkl, W.; Lemmer, U.; Feldmann, J.; Scherf, U.; Harth, E.; Gugel, A.; Mullen, K. *Phys. Rev. B* **1999**, *59*, 15346.
(11) Halls, J. J. M.; Pichler, K.; Friend, R. H.; Moratti, S. C.; Holmes, A. B. *Appl. Phys. Lett.* **1996**, *68*, 3120.
(12) Stubinger, T.; Brutting, W. *J. Appl. Phys.* **2001**, *90*, 3632.
(13) Barbu, E.; Tsibouklis, J. *Tetrahedron Lett.* **1996**, *37*, 5023.
(14) Brandsma, L.; Verkruijsse, H. D. *Synthesis* **1990**, 984.
(15) Based on Alami, M.; Ferri, F. *Tetrahedron Lett.* **1996**, *37*, 2763.
(16) Demas, J. N. *Excited-state lifetime measurements*; Academic Press: New York, 1983.
(17) Kenkre, V. M.; Parris, P. E.; Schmid, D. *Phys. Rev. B* **1985**, *32*, 4946.
(18) Rothberg, L. J.; Yan, M.; Papadimitrakopoulos, F.; Galvin, M. E.; Kwock, E. V.; Miller, T. M. *Synth. Met.* **1996**, *80*, 41.
(19) Scheidler, M.; Lemmer, U.; Kersting, R.; Karg, S.; Riess, W.; Cleve, B.; Mahrt, R. F.; Kurz, H.; Bassler, H.; Gobel, E. O.; Thomas, P. *Phys. Rev. B* **1996**, *54*, 5536.
(20) Ruseckas, A.; Theander, M.; Valkunas, L.; Andersson, M. R.; Inganas, O.; Sundstrom, V. *J. Lumin.* **1998**, *76*−*77*, 474.
(21) Sariciftci, N. S.; Smilowitz, L.; Heeger, A. J.; Wudl, F. *Science* **1992**, *258*, 1474.
(22) Brabec, C. J.; Zerza, G.; Cerullo, G.; De Silvestri, S.; Luzzati, S.; Hummelen, J. C.; Sariciftci, S. *Chem. Phys. Lett.* **2001**, *340*, 232.
(23) Parris, P. E.; Kenkre, V. M. *Chem. Phys. Lett.* **1982**, *90*, 342.
(24) Markov, D. E.; Hummelen, J. C.; Blom, P. W. M.; Sieval, A. B. Unpublished.

(25) Schlebusch, C.; Kessler, B.; Cramm, S.; Eberhardt, W. *Synth. Met.* **1996**, *77*, 151.

(26) Cantow, H.-J. *Polydiacetylenes*; Springer: Berlin, 1984.

(27) Hetzer, M.; Clausen-Schaumann, H.; Bayerl, S.; Bayerl, T. M.; Camps, X.; Vostrowsky, O.; Hirsch, A. *Angew. Chem., Int. Ed.* **1999**, *38*, 1962.

(28) Camps Camprubi, F. X. Thesis, University of Erlangen, Germany, 1998.

(29) The residual 4-pentynol could be removed by prolonged evaporation of volatile materials from the product (several hours in vacuo, using a rotary evaporator). Distillation is not a desirable process for purification of high-boiling diacetylenes because of their thermal instability.

(30) Prato, M.; Maggini, M. *Acc. Chem. Res.* **1998**, *31*, 519.

(31) These same effects were observed for F2C12 and have also been observed in other Prato adducts with comparable structures (van't Hof, P.; Valk, R.; Hummelen, J. C. To be published). There, it was also observed that the effect becomes more severe with increasing length of the alkyl chains. In a few control experiments, ^{13}C NMR measurements were done both in CS_2 and in $CDCl_3$, which confirmed that there was no unexpected overlap of the two aromatic CH signals due to the solvent used.

(32) del Pilar Carreón, M.; Burillo, G.; Fomina, L.; Ogawa, T. *Polym. J.* **1998**, *30*, 95.

(33) George, M.; Weiss, R. G. *Chem. Mater.* **2003**, *15*, 2879.

(34) Xu, S.-L.; Kang, S.-Z.; Gan, L.-B.; Zhang, L.; Wang, C.; Wan, L.-J.; Bai, C.-L. *Appl. Phys. A* **2003**, *77*, 757.